Universal Fluctuations of Single-Particle Diffusivity in a Quenched Environment

Takuma Akimoto,[1,*] Eli Barkai,[2] and Keiji Saito[3]
[1]Graduate School of Science and Technology, Keio University, Yokohama 223-8522, Japan
[2]Department of Physics, Bar Ilan University, Ramat-Gan 52900, Israel
[3]Department of Physics, Keio University, Yokohama 223-8522, Japan
(Received 23 April 2016; revised manuscript received 7 August 2016; published 27 October 2016)

Local diffusion coefficients in disordered materials such as living cells are highly heterogeneous. We consider finite systems with quenched disorder in order to investigate the effects of sample disorder fluctuations and confinement on single-particle diffusivity. While the system is ergodic in a single disorder realization, the time-averaged mean square displacement depends crucially on the disorder; i.e., the system is ergodic but non-self-averaging. Moreover, we show that the disorder average of the time-averaged mean square displacement decreases with the system size. We find a universal distribution for diffusivity in the sense that the shape of the distribution does not depend on the dimension. Quantifying the degree of the non-self-averaging effect, we show that fluctuations of single-particle diffusivity far exceed the corresponding annealed theory and also find confinement effects. The relevance for experimental situations is also discussed.

DOI: 10.1103/PhysRevLett.117.180602

Introduction—Anomalous diffusion, where the mean square displacement (MSD) does not depend linearly on time, unlike Brownian motion, has been extensively observed in complex systems such as disordered materials [1,2] and living cells [3–5]. One of the origins of anomalous diffusion is ascribed to a quenched random environment with highly heterogeneous local diffusivity. Such heterogeneous environments play a crucial role in the fluctuations of diffusivity observed in the one-dimensional diffusion of proteins on DNA [6,7] and diffusion in living cells [5]. In single-particle-tracking experiments, the trajectory $\boldsymbol{r}(t)$ of a tracer in a medium is recorded. One of the most common tools to quantify the diffusivity in experiments is the time-averaged MSD:

$$\overline{\delta^2(\Delta;t_m)} \equiv \frac{1}{t_m-\Delta}\int_0^{t_m-\Delta} dt' \delta\boldsymbol{r}_\Delta(t')^2, \qquad (1)$$

where t_m is the measurement time and $\delta\boldsymbol{r}_\Delta(t') \equiv \boldsymbol{r}(t'+\Delta)-\boldsymbol{r}(t')$. For Brownian motion in a homogeneous medium, the time-averaged MSD converges to the ensemble-averaged MSD $\overline{\delta^2} \sim 2dD\Delta$, where D is the diffusion coefficient and d is the space dimension. In strongly disordered systems, this equivalence can be broken, which is usually observed together with the onset of anomalous diffusion [8–11].

In the laboratory, diffusivity may represent either a "local" or "global" measurement. Consider, for example, normal Brownian motion in a homogeneous bounded system with size L. Short-time measurements ($t_m \ll L^2/D$) of the Brownian particles are local in the sense that the particles did not explore the phase space of the system. The opposite situation ($t_m \gg L^2/D$) implies a global measurement. In homogeneous systems, both the local and global measurements are identical, because $\overline{\delta^2} \sim 2dD\Delta$ for $\Delta \ll L^2/D$ and $\Delta \ll t_m$. However, a profoundly different scenario emerges for diffusion in strongly disordered systems, where the equivalence between local and global diffusivity breaks down in a nontrivial statistical way. In strongly disordered systems, the larger the system becomes, the more likely particles find extremely slow diffusive regions. Thus, as we will demonstrate, the global diffusivity may depend on the system size but not so for the local diffusivity. Both global and local measurements are practically important and widely measured. In particular, global measurements reveal anomalous diffusion for single mRNA in an *E. coli* cell [3], where the exploration of the cell is possible on the experimental time scale. On the other hand, local measurements are conducted for telomeres in the nucleus of the cell [12], where particles never encounter the system's boundary.

Anomalous diffusion in quenched environments is sometimes discussed by replacing the quenched disorder by an annealed one; i.e., the continuous-time random walk (CTRW) approximation is employed for both open [1,2] and closed systems [13,14]. However, when we look at finite disordered systems such as proteins on DNA or in living cells, it is not clear whether the annealed picture can accurately describe the underlying diffusion processes [5–7]. Therefore, it is desired to clarify properties of single-particle diffusion that are inherent in a quenched environment. Here, we consider the quenched trap model (QTM) [2] and derive several universal properties of diffusivity in the QTM. We show that fluctuations for global measurements of diffusivity in the QTM, among different realizations of the disorder, far exceed the corresponding fluctuations found for the CTRW. Thus, against common

belief, the annealed model does not capture the main ingredients of anomalous diffusion in the quenched environment. We show that the statistics of fluctuations of diffusivity is universal, because it is valid for any dimension. Confinement effects are also demonstrated. These will provide a basis to consider anomalous diffusion of single particles in finite systems with quenched disorder.

Model.—We consider a random walk on a quenched random energy landscape on a finite d-dimensional hypercubic lattice [2]. Quenched disorder means that when realizing the random energy landscape it does not change with time. The lattice constant is set to unity, and the number of lattice sites with different energies is L^d. At each lattice point, the depth $E > 0$ of an energy trap is randomly assigned. The depths are independent identically distributed random variables with an exponential distribution: $\rho(E) = T_g^{-1} \exp(-E/T_g)$. A particle can escape from a trap and jump to one of the nearest neighbors. The escape time $\tau_{\boldsymbol{r}}$ from a trap at site $\boldsymbol{r}$ follows the Arrhenius law, i.e., $\tau_{\boldsymbol{r}} = \tau_0 \exp(E_{\boldsymbol{r}}/T)$, where $E_{\boldsymbol{r}}$ is the depth of the energy at site $\boldsymbol{r}$, T the temperature, and τ_0 a typical time. Using $\rho(E)$ and the Arrhenius law, one can show that the probability density function (PDF) $\psi_\alpha(\tau)$ of trapping times follows

$$\int_\tau^\infty d\tau' \psi_\alpha(\tau') = \left(\frac{\tau}{\tau_0}\right)^{-\alpha} (\tau \geq \tau_0) \tag{2}$$

with $\alpha \equiv T/T_g$ [15]. Thus, the mean trapping time diverges for $\alpha \leq 1$, which leads to anomalous behaviors [2,16–22]. Note that the sample mean trapping time $\mu = \sum_{\boldsymbol{r}} \tau_{\boldsymbol{r}}/L^d$ for a fixed disorder never diverges when $L < \infty$. Thus, one can define the sampling time as the time scale on which coverage of the system's phase space is reached, e.g., $t_{\rm sam} \propto L^2$ for $d = 1$ and $t_{\rm sam} \propto L^d$ for $d > 1$ in a simple random walk [23,24], where we ignored a logarithmic contribution. The statistics of the time-averaged MSD is now classified into two regimes for the measurement time t_m: local measurements ($t_m \ll t_{\rm sam}$) and global measurements ($t_{\rm sam} \ll t_m$). For global measurements of the time-averaged MSD, we consider small and large Δ regimes because of the confinement effect.

Let $P_{\boldsymbol{r}}$ be the probability of finding a particle at site $\boldsymbol{r}$. Except for the boundary, the master equation for the ith disorder realization $\tau_{\boldsymbol{r}}^{(i)}$ is given by

$$\frac{dP_{\boldsymbol{r}}}{dt} = \frac{1}{2d} \sum_{\boldsymbol{r}'} \frac{P_{\boldsymbol{r}'}}{\tau_{\boldsymbol{r}'}^{(i)}} - \frac{P_{\boldsymbol{r}}}{\tau_{\boldsymbol{r}}^{(i)}}, \tag{3}$$

where the sum is over the nearest-neighbor sites. We consider global measurements for two boundary conditions: periodic and reflecting. In both cases, when we take long measurements ($t_m \gg 1$), the finite system reaches an equilibrium state:

$$P_{\boldsymbol{r}}^{\rm eq} = \frac{\tau_{\boldsymbol{r}}^{(i)}}{L^d \mu_i}, \tag{4}$$

where $\mu_i = \sum_{\boldsymbol{r}} \tau_{\boldsymbol{r}}^{(i)}/L^d$ is the sample mean trapping time.

Universal distribution of diffusion coefficient for global measurement in a small Δ regime.—When Δ is small, the time-averaged MSD is not sensitive to the type of boundary condition. Here, we use the periodic boundary condition. Since processes in finite size systems are ergodic [see Eq. (11)], $\overline{\delta^2(\Delta; t_m)}$ can be replaced by the ensemble-averaged MSD with the equilibrium initial condition for global measurements. The MSD for the ith disorder realization increases as $\langle \delta \boldsymbol{r}_\Delta(0)^2 \rangle_{\rm eq} = \langle N_\Delta \rangle_{\rm eq}$, where $\langle N_\Delta \rangle_{\rm eq}$ is the mean number of jumps until time Δ and $\langle \cdot \rangle_{\rm eq}$ implies the equilibrium initial ensemble. Thus, we have

$$\overline{\delta^2(\Delta; t_m)} \xrightarrow{t_m \to \infty} \langle \delta \boldsymbol{r}_\Delta(0)^2 \rangle_{\rm eq} = \langle N_\Delta \rangle_{\rm eq} = \frac{\Delta}{\mu_i} \tag{5}$$

for a single disorder realization, because the rate that a particle jumps does not change in time with the aid of equilibration (see Supplemental Material for the derivation [25]). This result is exact for any $\Delta > 0$. We note that this average is taken over equilibrium initial conditions and thermal histories but not over disorder.

Now, we consider the effect of disorder on the diffusivity. Since the diffusion is normal, we define the diffusion coefficient for a single disorder realization i as $D_i \equiv \langle \delta \boldsymbol{r}_\Delta(0)^2 \rangle_{\rm eq}/(2d\Delta)$, and hence $D_i = 1/(2d\mu_i)$. When the mean trapping time $\langle \tau \rangle \equiv \int_0^\infty \tau \psi(\tau) d\tau$ is finite ($\alpha > 1$), we have $\mu_i \to \langle \tau \rangle$ ($L \to \infty$) by the law of large numbers. In this limit, the diffusion coefficient does not depend on the disorder realization. Hence, the diffusion coefficient is self-averaging (SA) [2].

When the mean trapping time diverges ($\alpha \leq 1$), the law of large numbers breaks down. Instead, the PDF of the normalized sum of $\tau_{\boldsymbol{r}}^{(i)}$ follows the one-sided Lévy distribution [26]:

$$\frac{\sum_{\boldsymbol{r}} \tau_{\boldsymbol{r}}^{(i)}}{(L^d)^{1/\alpha}} \Rightarrow X_\alpha \, (L \to \infty), \tag{6}$$

where X_α is a random variable following the one-sided Lévy distribution of index α. The PDF of X_α denoted by $l_\alpha(x)$ with $x > 0$ is given by [26]

$$l_\alpha(x) = -\frac{1}{\pi x} \sum_{k=1}^\infty \frac{\Gamma(k\alpha + 1)}{k!} (-cx^{-\alpha})^k \sin(k\pi\alpha), \tag{7}$$

where $c = \Gamma(1 - \alpha)\tau_0^\alpha$ is a scale parameter. Here, we define the inverse Lévy distribution as the PDF of X_α^{-1}:

$$g_\alpha(y) = -\frac{1}{\pi y} \sum_{k=1}^\infty \frac{\Gamma(k\alpha + 1)}{k!} (-cy^\alpha)^k \sin(k\pi\alpha). \tag{8}$$

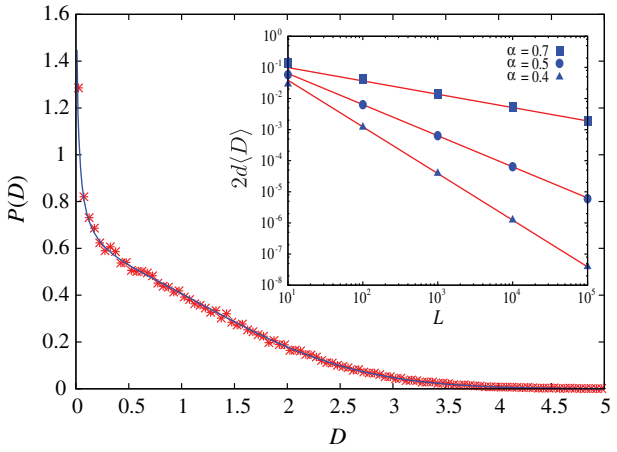

FIG. 1. Distribution of the diffusion coefficients for different disorder realizations ($T = 1$ and $T_g = 1.5$). The crosses are the results of the numerical simulation ($d = 1$ and $L = 10^4$). The mean of the PDF is set to unity. The solid line is the inverse Lévy distribution [Eq. (8)]. The inset shows the disorder average of diffusion coefficients as a function of the system size L for several $\alpha = T/T_g$. Here, the symbols are the results of numerical simulations, and the solid lines are the theoretical curves [Eq. (9)]. In both numerical simulations, we calculated the diffusion coefficients ($2dD = 1/\mu^i$) for different disorder realizations by Monte Carlo simulations (see Supplemental Material [25] for finite time simulations).

Because the diffusion coefficient is given by $D_i = (L^d)^{1-1/\alpha} X_\alpha^{-1}/(2d)$, the PDF of D_i is described by the inverse Lévy distribution, and hence D_i depends crucially on the sample of the disorder realization. As discussed later, these fluctuations are much larger if compared with the annealed model. As shown in Fig. 1, our rigorous result for the asymptotic distribution of the diffusion coefficients is in good agreement with the numerical simulations. Surprisingly, the inverse Lévy distribution is a universal distribution of the diffusion coefficient in the sense that it is exact for any dimension. Using the first moment of the inverse Lévy distribution [25], we obtain the exact asymptotic behavior of the disorder average of the diffusion coefficient:

$$\langle D \rangle_{\rm dis} \sim \frac{L^{d(1-1/\alpha)}\Gamma(\alpha^{-1})}{2d\alpha\tau_0\Gamma(1-\alpha)^{1/\alpha}}, \tag{9}$$

where $\langle\cdot\rangle_{\rm dis}$ means the disorder average, i.e., the average taken from many trajectories obtained under different disorder realizations. We confirm that this asymptotic result is valid for large L as presented in Fig. 1. To develop some physical interpretations for Eq. (9), we note that, when the system size is increased, one finds deeper and deeper traps, these in turn tend to localize the particle for long times, and hence diffusivity is decreased as the system size is increased. This effect vanishes as $\alpha \to 1$. Since the system is ergodic as will be shown below, the time-averaged MSD becomes $\langle\overline{\delta^2(\Delta; t_m)}\rangle_{\rm dis} \to 2d\langle D\rangle_{\rm dis}\Delta$ as $t_m \to \infty$ (see Fig. S3 in Supplemental Material [25]).

Ergodicity.—To investigate the ergodic properties of the disordered system, we consider the ergodicity breaking (EB) parameter [27] defined by

$$\mathrm{EB}(t_m; \Delta) \equiv \frac{\langle\overline{\delta^2(\Delta; t_m)}^2\rangle_{\rm path} - \langle\overline{\delta^2(\Delta; t_m)}\rangle^2_{\rm path}}{\langle\overline{\delta^2(\Delta; t_m)}\rangle^2_{\rm path}}, \tag{10}$$

where $\langle\cdot\rangle_{\rm path}$ implies an ensemble average using many different trajectories. Here we note that we consider a single disorder realization and that the definition Eq. (10) holds also for the CTRW [27]. If the EB parameter goes to zero, the time-averaged MSD for a single disorder realization converges to a constant; that is, the process is ergodic: $\overline{\delta^2(\Delta; t_m)} \to \langle \delta \boldsymbol{r}_\Delta(0)^2\rangle_{\rm eq}$ for $t_m \to \infty$. In the CTRW, the EB parameter is not zero even when t_m goes to infinity [14,27]. For global measurements, the EB parameter for a single disorder realization decays as

$$\mathrm{EB}(t_m; \Delta) \sim \frac{4\Delta}{3dt_m} \quad (t_m \to \infty \quad \text{and} \quad \Delta \gg 1), \tag{11}$$

which means that the system is ergodic (see Supplemental Material [25] for the derivation). This statement becomes invalid for an infinite system ($L = \infty$), because there is no equilibrium state [19].

Self-averaging.—Next, we propose another quantity characterizing the SA property. The SA parameter for the time-averaged MSD is defined as

$$\mathrm{SA}(t_m, L; \delta \boldsymbol{r}^2_\Delta) \equiv \frac{\langle\overline{\delta^2(\Delta; t_m)}^2\rangle_{\rm dis} - \langle\overline{\delta^2(\Delta; t_m)}\rangle^2_{\rm dis}}{\langle\overline{\delta^2(\Delta; t_m)}\rangle^2_{\rm dis}}. \tag{12}$$

Because the system is ergodic for finite L, the SA parameter becomes

$$\mathrm{SA}(t_m, L; \delta \boldsymbol{r}^2_\Delta) \xrightarrow[t_m \to \infty]{} \frac{\langle 1/\mu_i^2\rangle_{\rm dis} - \langle 1/\mu_i\rangle^2_{\rm dis}}{\langle 1/\mu_i\rangle^2_{\rm dis}}. \tag{13}$$

The difference between EB and SA parameters is in their averaging procedures. For the former we use a single disordered system and average over paths $\langle\cdot\rangle_{\rm path}$, while for the latter we average over many realizations of disorder $\langle\cdot\rangle_{\rm dis}$. Using the first and the second moment of $1/\mu_i$ obtained in Supplemental Material [25], we have the SA parameter

$$\lim_{L\to\infty}\lim_{t_m\to\infty} \mathrm{SA}(t, L; \delta \boldsymbol{r}^2_\Delta) = \begin{cases} 0 & (\alpha > 1) \\ \frac{\alpha\Gamma(\frac{2}{\alpha})}{\Gamma(\frac{1}{\alpha})^2} - 1 & (\alpha \le 1). \end{cases} \tag{14}$$

The SA parameter becomes zero when the process is SA. Hence, the process is not SA for $\alpha < 1$, whereas it is ergodic when $L < \infty$. The results obtained so far show striking differences if compared with the CTRW. In the

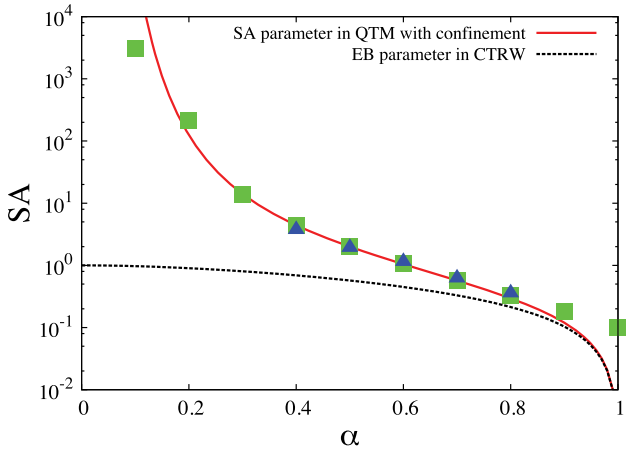

FIG. 2. Self-averaging parameter as a function of α. The squares and the triangles are obtained by Monte Carlo simulations of Eq. (13) ($d = 1$ and $L = 10^3$) and the numerical simulation of dynamics of the QTM ($d = 3$, $L = 10$, and $t_m = 10^7$ for $\alpha = 0.8$ and 10^8 for other cases), respectively. The solid and the dotted lines are the SA parameter in the QTM [Eq. (14)] and the EB parameter in the CTRW, which is given by $2\Gamma(1+\alpha)^2/\Gamma(2\alpha+1) - 1$ [27], respectively.

CTRW one finds ergodicity breaking [14,27–29], while so far we have found non-SA. While there is no quenched disorder in the dynamics of the CTRW, the EB parameter in the CTRW corresponds to the SA parameter in the QTM. Thus, it becomes meaningful to compare between the magnitude of these fluctuations, and we show that the non-SA effect is much stronger than the EB effects (see Fig. 2). The difference between the CTRW and QTM is the fact that waiting time distributions at all lattice points are identical in the CTRW, and thus the CTRW is homogeneous. Furthermore, the distribution of the diffusion constant in the QTM is not bounded at $D = 0$ (see Fig. 1), which implies a heavy statistical weight for very slow particles. Because this effect is not found for the annealed model, quenched models lead to surprisingly large fluctuations. Finally, in the CTRW, diffusivity depends on the measurement time, i.e., a phenomenon called aging [8,27,29,30]. On the other hand, the system size controls the long-time statistics of the diffusion coefficient in the QTM with confinement, e.g., Eq. (9).

Fluctuations in global measurement in a large Δ *regime.*—For large Δ, effects of the boundary on the MSD are inevitable. Thus, the MSD converges to a constant as $\Delta \to \infty$ due to the confinement. Here, we consider fluctuations of the time-averaged position due to disorder realizations. Because the system is ergodic, the SA parameter for the position in the long-time limit ($t \to \infty$) is given by

$$\mathrm{SA}(t_m, L; \boldsymbol{r}) \equiv \frac{\langle \bar{\boldsymbol{r}}^2 \rangle_{\mathrm{dis}} - \langle \bar{\boldsymbol{r}} \rangle_{\mathrm{dis}}^2}{\langle \bar{\boldsymbol{r}} \rangle_{\mathrm{dis}}^2} \to \frac{\langle \langle \boldsymbol{r} \rangle_{\mathrm{eq}}^2 \rangle_{\mathrm{dis}} - \langle \langle \boldsymbol{r} \rangle_{\mathrm{eq}} \rangle_{\mathrm{dis}}^2}{\langle \langle \boldsymbol{r} \rangle_{\mathrm{eq}} \rangle_{\mathrm{dis}}^2}, \tag{15}$$

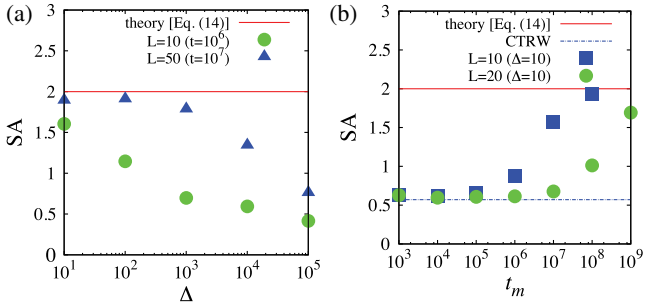

FIG. 3. Effects of confinement in sample-to-sample fluctuations ($\alpha = 0.5$). SA parameters for the time-averaged MSD as a function of (a) the lag time ($d = 1$) and (b) the measurement time ($d = 3$). The solid and dashed lines represent Eq. (14) and the EB parameter in the CTRW, respectively. Symbols are the results of numerical simulations, where we simulated dynamics of the QTM (see Supplemental Material [25]).

where $\bar{\boldsymbol{r}} \equiv \int_0^t \boldsymbol{r}(t')dt'/t$. Using methods similar to those presented in Ref. [31], we show in Supplemental Material [25] that the SA parameter for the position becomes

$$\lim_{L\to\infty} \lim_{t_m\to\infty} \mathrm{SA}(t_m, L; \boldsymbol{r}) = \begin{cases} 0 & (\alpha > 1) \\ \frac{1-\alpha}{3} & (\alpha \le 1). \end{cases} \tag{16}$$

Thus, the non-SA behavior of the position under confinement appears for $\alpha < 1$. Unlike the SA parameter for the time-averaged MSD, that for the position does not blow up when $\alpha \to 0$.

As shown in Fig. 3(a), the SA parameter of the time-averaged MSD depends on the lag time Δ and saturates due to the confinement. Hence, the time-averaged MSD is also non-SA under confinement for a large Δ regime. We note that the EB parameter does not depend on Δ in the CTRW with confinement [13,14].

Local measurements $\Delta \ll t_m \ll t_{\mathrm{sam}}$.—In local measurements, trajectories of particles are not exploring the full extent of the system, and one may regard the process as a motion in an infinite system. For $d \ge 2$, the CTRW model is a valid description of the QTM. This implies that we may observe a transition in the SA parameter as the measurement time is increased. As shown in Fig. 3(b), for local measurements $t_m \ll t_{\mathrm{sam}}$, we get the CTRW-like description, while increasing t_m finally crossing to the limit $t_m \gg t_{\mathrm{sam}}$ we observe the behavior predicted here in Eq. (14). The SA parameter increases with measurement time in this example, which is a general trend in the QTM but not in the annealed model.

Discussion.—We analytically showed ergodicity and non-SA properties in a d-dimensional QTM with a finite system size. The non-SA effects lead to universal fluctuations of diffusivity; that is, the PDF of the diffusion coefficient follows the inverse Lévy distribution in arbitrary dimension. The inverse Lévy distribution stems from the Lévy distribution, which is a universal distribution for the

sum of trapping times. Therefore, it will be found in other models beyond the QTM like the random comb model and the results are truly universal. We have also quantified the degree of the non-SA property by the SA parameter. The fluctuations of diffusivity in quenched environments are much larger than those in the annealed model. Note that the limits $t_m \to \infty$ and $L \to \infty$ in the SA parameter are not commutable. This is because partial equilibrium in the infinite system does not hold, as shown in Refs. [32,33]. Moreover, when we look at $\langle \delta \boldsymbol{r}_\Delta(0)^2 \rangle_{\rm dis}$ with a nonequilibrium initial condition, it shows subdiffusion for a small Δ regime (see Supplemental Material [25]).

In an experiment, self-averaging can be tested by repeating experiments in many environments, e.g., different cells of the same type in single-molecule experiments. For the QTM with a finite size, the process is non-SA but ergodic. In single-particle-tracking experiments, one might find fluctuations of diffusivity in one cell and in addition those in between different cells of the same type. Thus, our work opens the way to quantify fluctuations within a cell (EB parameter) and among different cells (SA parameter).

The time-averaged MSD depends on both the lag time and the measurement time (unlike the ensemble average). The relative magnitude of these two times compared to $t_{\rm sam}$ yields rich behaviors compared to normal diffusion processes. For long measurement times, compared with $t_{\rm sam}$, diffusivity decreases with the system size L [Eq. (9)], since as L is increased the trapping times encountered by the particle become longer.

T. A. and K. S. were supported by JSPS KAKENHI Grants No. 26800204 and No. JP25103003, respectively. E. B. acknowledges the Israel Science Foundation.

*akimoto@keio.jp

[1] H. Scher and E. W. Montroll, Phys. Rev. B **12**, 2455 (1975).
[2] J. Bouchaud and A. Georges, Phys. Rep. **195**, 127 (1990).
[3] I. Golding and E. C. Cox, Phys. Rev. Lett. **96**, 098102 (2006).
[4] A. Weigel, B. Simon, M. Tamkun, and D. Krapf, Proc. Natl. Acad. Sci. U.S.A. **108**, 6438 (2011).
[5] C. Manzo, J. A. Torreno-Pina, P. Massignan, G. J. Lapeyre, Jr., M. Lewenstein, and M. F. Garcia Parajo, Phys. Rev. X **5**, 011021 (2015).
[6] A. Granéli, C. C. Yeykal, R. B. Robertson, and E. C. Greene, Proc. Natl. Acad. Sci. U.S.A. **103**, 1221 (2006).
[7] Y. M. Wang, R. H. Austin, and E. C. Cox, Phys. Rev. Lett. **97**, 048302 (2006).
[8] R. Metzler, J.-H. Jeon, A. G. Cherstvy, and E. Barkai, Phys. Chem. Chem. Phys. **16**, 24128 (2014).
[9] F. Höfling and T. Franosch, Rep. Prog. Phys. **76**, 046602 (2013).
[10] Y. Meroz and I. M. Sokolov, Phys. Rep. **573**, 1 (2015).
[11] T. Akimoto and T. Miyaguchi, Phys. Rev. E **87**, 062134 (2013).
[12] I. Bronstein, Y. Israel, E. Kepten, S. Mai, Y. Shav-Tal, E. Barkai, and Y. Garini, Phys. Rev. Lett. **103**, 018102 (2009).
[13] T. Neusius, I. M. Sokolov, and J. C. Smith, Phys. Rev. E **80**, 011109 (2009).
[14] T. Miyaguchi and T. Akimoto, Phys. Rev. E **87**, 032130 (2013).
[15] F. Bardou, J.-P. Bouchaud, A. Aspect, and C. Cohen-Tannoudji, *Levy Statistics and Laser Cooling: How Rare Events Bring Atoms to Rest* (Cambridge University Press, Cambridge, England, 2002).
[16] J. Machta, J. Phys. A **18**, L531 (1985).
[17] C. Monthus and J.-P. Bouchaud, J. Phys. A **29**, 3847 (1996).
[18] S. Burov and E. Barkai, Phys. Rev. Lett. **98**, 250601 (2007); **106**, 140602 (2011).
[19] T. Miyaguchi and T. Akimoto, Phys. Rev. E **83**, 031926 (2011).
[20] P. Massignan, C. Manzo, J. A. Torreno-Pina, M. F. García-Parajo, M. Lewenstein, and G. J. Lapeyre, Phys. Rev. Lett. **112**, 150603 (2014).
[21] T. Miyaguchi and T. Akimoto, Phys. Rev. E **91**, 010102 (2015).
[22] L. Luo and L.-H. Tang, Phys. Rev. E **92**, 042137 (2015).
[23] C. S. Yokoi, A. Hernández-Machado, and L. Ramírez-Piscina, Phys. Lett. A **145**, 82 (1990).
[24] A. M. Nemirovsky, H. O. Mártin, and M. D. Coutinho-Filho, Phys. Rev. A **41**, 761 (1990).
[25] See Supplemental Material at http://link.aps.org/supplemental/10.1103/PhysRevLett.117.180602 for the moments of the inverse Lévy distribution, the derivation of the EB parameter in a single disorder realization, the derivation of the SA parameter for position, the PDF of diffusion coefficients for finite time simulations, and the numerical method.
[26] W. Feller, *An Introduction to Probability Theory and its Applications*, 2nd ed. (Wiley, New York, 1971), Vol. 2.
[27] Y. He, S. Burov, R. Metzler, and E. Barkai, Phys. Rev. Lett. **101**, 058101 (2008).
[28] J.-P. Bouchaud, J. Phys. I (France) **2**, 1705 (1992).
[29] A. Lubelski, I. M. Sokolov, and J. Klafter, Phys. Rev. Lett. **100**, 250602 (2008).
[30] J. H. P. Schulz, E. Barkai, and R. Metzler, Phys. Rev. Lett. **110**, 020602 (2013).
[31] A. Rebenshtok and E. Barkai, Phys. Rev. Lett. **99**, 210601 (2007); J. Stat. Phys. **133**, 565 (2008).
[32] L. R. G. Fontes, M. Isopi, and C. Newman, Ann. Probab. **30**, 579 (2002).
[33] E. M. Bertin and J.-P. Bouchaud, Phys. Rev. E **67**, 026128 (2003).